

Cosmological data analysis of $f(R)$ gravity models

Z. Gironés^{*}, A. Marchetti[†], O. Mena[‡], C. Peña-Garay[§] and N. Rius[¶]

*Depto. de Física Teórica, IFIC, Universidad de Valencia-CSIC
Edificio de Institutos de Paterna, Apt. 22085, 46071 Valencia, Spain*

ABSTRACT: A class of well-behaved modified gravity models with long enough matter domination epoch and a late-time accelerated expansion is confronted with SNIa, CMB, SDSS, BAO and $H(z)$ galaxy ages data, as well as current measurements of the linear growth of structure. We show that the combination of geometrical probes and growth data exploited here allows to rule out $f(R)$ gravity models, in particular, the logarithmic of curvature model. We also apply solar system tests to the models in agreement with the cosmological data. We find that the exponential of the inverse of the curvature model satisfies all the observational tests considered and we derive the allowed range of parameters. Current data still allows for small deviations of Einstein gravity. Future, high precision growth data, in combination with expansion history data, will be able to distinguish tiny modifications of standard gravity from the Λ CDM model.

KEYWORDS: Modified Gravity, Linear perturbation theory.

^{*}girones@ific.uv.es

[†]alida.marchetti@unimi.it

[‡]omena@ific.uv.es

[§]carlos.penya@ific.uv.es

[¶]nuria@ific.uv.es

Contents

1. Introduction	1
2. $f(R)$ Models	2
2.1 Background evolution	3
2.2 Linear growth rate $\delta(a)$	4
3. Cosmological data used in the analysis	6
3.1 The Supernova Union Compilation	7
3.2 CMB first acoustic peak	7
3.3 BAOs	7
3.4 Galaxy ages	8
3.5 Growth factor	8
4. Analysis of cosmological models	9
4.1 Model H1: $f(R) = \alpha R^n$ ($\alpha < 0$, $0 < n < 1$)	10
4.2 Model H2: $f(R) = R(\log(\alpha R))^q - R$ ($q > 0$)	10
4.3 Model H3: $f(R) = R \exp(q/R) - R$	11
4.4 Model H4: $f(R) = \alpha R^2 - \Lambda$ ($\alpha \Lambda \ll 1$)	12
5. Solar system constraints	12
6. Discussion	15

1. Introduction

Astronomical observations have led to the inference that our universe is approximately flat and its mass-energy budget consists of 5% ordinary matter, 22% non-baryonic dark matter, plus a dominant negative-pressure component that accelerates the Hubble expansion [1–5]. The current accelerated expansion of the universe reveals new physics missing from our universe’s picture, and it constitutes the fundamental key to understand the fate of the universe.

The most economical description of the cosmological parameters attributes the negative-pressure *dark energy* component to a cosmological constant (CC) in Einstein’s equations. The CC represents an invariable vacuum energy density that assumes a greater importance as the Universe expands. The equation of state w of the dark energy component in the CC case is constant and $w = P_{de}/\rho_{de} = -1$, where P_{de} and ρ_{de} denote dark energy pressure and energy density, respectively. However, when computing the vacuum energy density

from the quantum field theory approach, the naively expected value exceeds the measured one by 123 orders of magnitude and it needs to be cancelled by extreme fine-tuning. This is the so-called CC problem. A related problem is the so called *why now?* or *coincidence* problem, i.e. why the dark matter and dark energy contributions to the energy budget of the universe are similar at this precise moment of the cosmic history.

A dynamical alternative attributes the accelerated expansion to a cosmic scalar field, *quintessence* [6–11], that changes with time and varies across space, slowly approaching its ground state. In this case, the equation of state w could vary over time. However, quintessence models are not better than the CC scenario as regards fine-tuning, since there is no symmetry that explains the tiny value of the potential at its ground state.

There exists another possible scenario, in which the gravitational sector is modified, as an alternative to explain the observed cosmic acceleration. Although this requires the modification of Einstein’s equations of gravity on very large distances [12], or on small curvatures [13–15], this is not unexpected for an effective 4-dimensional description of higher dimensional theories. *Modifications of gravity* have been examined in the context of accelerated expansion. The proposed modified gravity models have extra spatial dimensions or an action which is non linear in the curvature scalar, that is, these models include extensions of the Einstein-Hilbert action, for instance, to higher derivative theories [16], scalar-tensor theories or generalized functions of the Ricci scalar $f(R)$.

Among a plethora of $f(R)$ models, a recent study [17] has identified those cosmologically acceptable, i.e. models with a standard matter era followed by an accelerated attractor. We focus here on the cosmological bounds on these *viable* $f(R)$ models. We use recent SNIa, BAO, CMB and $H(z)$ galaxy ages data to constrain the background evolution in this class of $f(R)$ models. We exploit as well current measurements of the linear growth of structure, which provides us an additional test to be combined with the background probes. The $f(R)$ models which are not ruled out by the global cosmological analysis will be examined under solar system constraints.

The structure of the paper is as follows. We start in Sec. 2 specifying the class of modified gravity models explored here, as well as the equations which describe the background evolution and the linear perturbation theory in a generic $f(R)$ model. Section 3 contains a description of the different cosmological data sets used in the analysis performed here. Our results are presented in Sec. 4. We describe the solar system constraints in Sec. 5. We summarize our results, draw our conclusions and discuss future work in Sec. 6.

2. $f(R)$ Models

We investigate the simplest family of modified gravity models, obtained by adding to the usual Hilbert-Einstein Lagrangian some function $f(R)$ of the Ricci scalar R , with an action given by

$$\mathcal{L} = \int d^4x (R + f(R))\sqrt{g} + \mathcal{L}_{matter} . \quad (2.1)$$

Here we analyse $f(R)$ models which are cosmologically viable, i.e., models which predict a matter dominated period followed later by an accelerated expansion epoch. In the matter

domination era the effective equation of state is close to $\omega_{eff} = 0$ and the scale factor a grows with time as $a(t) \sim t^{2/3}$.

The authors of [17] have explored the general conditions for the cosmological viability of $f(R)$ models in the context of a flat, homogeneous and isotropic background. The cosmological behaviour of $f(R)$ models can be characterized by studying the $m(r)$ curve on the (m, r) plane [17], where

$$m = \frac{Rf_{RR}}{1 + f_R} ; \quad r = -\frac{R(1 + f_R)}{R + f} , \quad (2.2)$$

and $f_R \equiv df/dR$. A given $f(R)$ model will have a standard matter dominated period followed by a late time accelerated era if the conditions $m(r) \approx +0$ and $dm/dr > -1$ at $r \approx -1$ are satisfied, respectively.

Reference [17] shows that all $f(R)$ models with an accelerated global attractor belong to four classes, two of which can be cosmologically acceptable: models of Class II, asymptotically equivalent to the Λ CDM model ($\omega_{eff} = -1$), and models of Class IV, which have a non-phantom final accelerated expansion period ($\omega_{eff} > -1$). In practice, there are not $f(R)$ models belonging to Class IV, unless they are built by hand from a well-behaved $m(r)$ function. There are other type of models, as those from Class III, which have an unstable matter era followed by a phantom acceleration ($\omega_{eff} < -1$). These Class III models are generally ruled out by observations, although a more careful numerical analysis is needed. We focus here on the Class II models of Ref. [17], studying the following four cases:

$$H1 : f(R) = \alpha R^n , \alpha < 0, 0 < n < 1 ; \quad (2.3)$$

$$H2 : f(R) = R [\log(\alpha R)]^q - R , (q > 0) ; \quad (2.4)$$

$$H3 : f(R) = R \exp(q/R) - R ; \quad (2.5)$$

$$H4 : f(R) = \alpha R^2 - \Lambda , (\alpha \Lambda \ll 1) . \quad (2.6)$$

2.1 Background evolution

The field equations, which can be obtained varying the action (2.1) with respect to $g_{\mu\nu}$, read

$$(1 + f_R)R_{\mu\nu} - \frac{g_{\mu\nu}}{2}(R + f - 2\Box f_R) - \nabla_\mu \nabla_\nu f_R = 8\pi G T_{\mu\nu} . \quad (2.7)$$

The metric we take is of the form of a flat Friedman Robertson Walker (FRW) background $ds^2 = -dt^2 + a(t)^2 \sum_{i=1}^3 (dx^i)^2$, with $a(t)$ the scale factor. The Friedmann equation is given by

$$H^2 - (H^2 + aHH')f_R + aH^2 f'_R + \frac{1}{6}f = \frac{8\pi G}{3}\rho \quad (2.8)$$

where $' \equiv d/da$, $H = (da/dt)/a$ denotes the Hubble expansion rate, ρ refers to the total cold dark matter energy density and $R = 6(2H^2 + aHH')$. The present dark matter energy density has been fixed to $\Omega_m^0 = 0.24$ (when not treated as a free parameter), accordingly to a recent fit to cosmological data [2]. We have integrated numerically the background equation (2.8) for the four $f(R)$ Class II functions given by Eqs. (2.3), (2.4), (2.5) and (2.6).

We have determined the ranges of the free parameters which lead to a value of the Hubble constant within its current 1σ range $H_0 = 74.2 \pm 3.6$ km/s/Mpc [18]. Figure I shows the results for the Hubble parameter $H(a)$ for the four different $f(R)$ models explored here. As a comparison, we depict as well the Hubble rate for a flat universe with a CC (Λ CDM model)*. The H_0 values for the choice of parameters used in Fig. I are 76.7, 75.4, 70.6 and 71.0 km/s/Mpc for $f(R) = \alpha R^n$, $f(R) = R(\log(\alpha R))^q - R$, $f(R) = R \exp(q/R) - R$ and $f(R) = \alpha R^2 - \Lambda$, respectively.

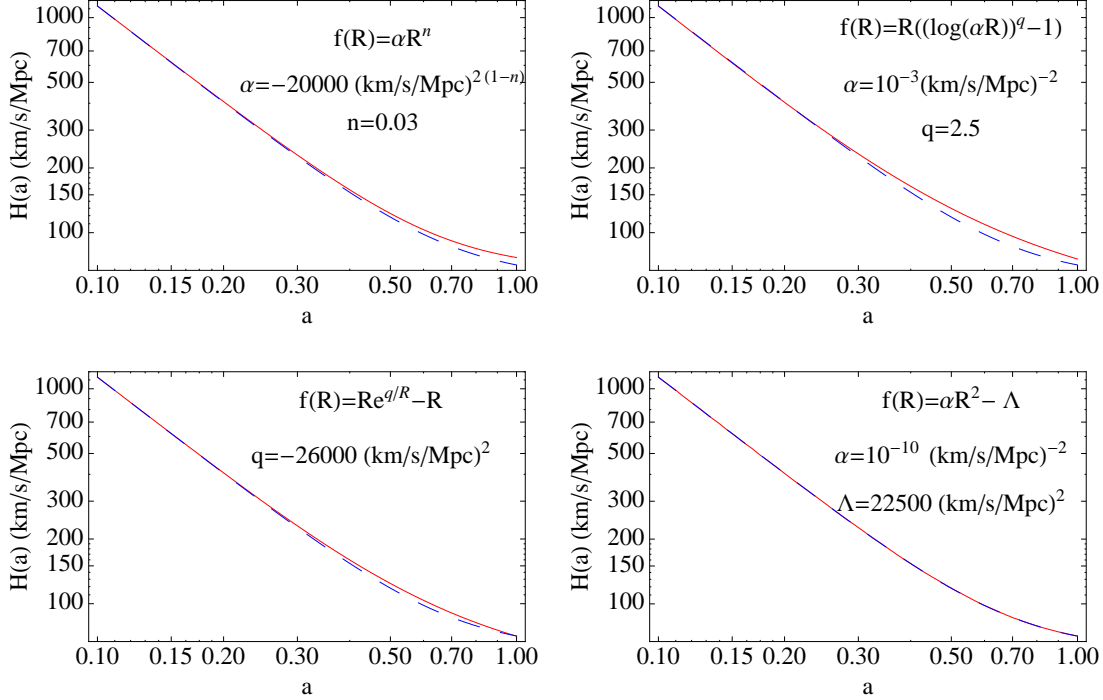


Figure I: Expansion history of various $f(R)$ models. The red solid curves depict the Hubble rate versus the scale factor for the $f(R)$ models explored in this work. The parameters were chosen so to have an acceptable expansion history. We have added the Λ CDM model $H(a)$ (blue dashed curve) for comparison.

2.2 Linear growth rate $\delta(a)$

We consider scalar linear perturbations around a flat FRW background in the Newtonian gauge

$$ds^2 = -(1 + 2\Psi)dt^2 + a(t)^2(1 + 2\Phi) \sum_{i=1}^3 (dx^i)^2. \quad (2.9)$$

The perturbations to the metric are the Newtonian potential Ψ and the perturbation to the spatial curvature Φ . Since we are working in the Jordan frame, in which matter is minimally

*The Hubble rate for the Λ CDM model, neglecting the radiation contribution, reads $H(a) = H_0 \sqrt{\Omega_m^0 a^{-3} + (1 - \Omega_m^0)}$.

coupled, the conservation equations for the cold dark matter component have the same form than in general relativity. At first order in the perturbations, the conservation equations read

$$\begin{aligned}\dot{\delta} &= 3\dot{\Phi} - \theta ; \\ \dot{\theta} &= -H\theta + \left(\frac{k}{a}\right)^2 \Psi ,\end{aligned}\tag{2.10}$$

where $\dot{}$ means derivative with respect to t , δ is the cold dark matter overdensity and θ is the dark matter (comoving) peculiar velocity divergence. For subhorizon modes ($k \gtrsim aH$), and in the quasi-static limit[†], the perturbed $0-0$ and $i-j$ ($i \neq j$) components of the Einstein equations read

$$2\left(\frac{k}{a}\right)^2 \left[\Phi(1 + f_R) - f_{RR} \left(\frac{k}{a}\right)^2 (\Psi - 2\Phi) \right] = -8\pi G \rho \delta ;\tag{2.11}$$

$$\Psi = \left(\frac{1 - 2Q}{1 - Q}\right) \Phi ,\tag{2.12}$$

where we have set the anisotropic stress of cold dark matter to zero, ρ refers to the cold dark matter energy density and we have neglected the radiation contribution. The factor Q is defined as

$$Q(k, a) = -2 \left(\frac{k}{a}\right)^2 \frac{f_{RR}}{1 + f_R} .\tag{2.13}$$

By substituting the equation for the $i-j$ component into the one for the $0-0$ component one gets the modified Poisson equation

$$\Phi = \frac{-8\pi G}{\left(\frac{k}{a}\right)^2 (1 + f_R)} \rho \delta \left(\frac{1 - Q}{2 - 3Q}\right) ,\tag{2.14}$$

which reduces to the standard one if $f_R = 0$. The growth factor equation is obtained by combining Eqs. (2.10) and Eq. (2.14), see also Ref. [19]:

$$\delta'' + \delta' \left(\frac{3}{a} + \frac{H'}{H}\right) - \frac{3\Omega_m(a)}{(H/H_0)^2 (1 + f_R)} \frac{1 - 2Q}{2 - 3Q} \frac{\delta}{a^2} = 0 ,\tag{2.15}$$

where $' \equiv d/da$, $\Omega_m(a) = \Omega_m^0 a^{-3}$ and δ is normalized such that $\delta \rightarrow a$ when $a \rightarrow 0$. In general relativity, the factor Q given by Eq. (2.13) is zero and therefore the linear density growth is scale independent for all dark energy models. However, for $f(R)$ models, the scale dependent $Q(k, a)$ induces a nontrivial scale dependence of the growth δ .

We illustrate this scale dependence of the growth factor in Fig. II, where it is shown the present value of the matter overdensity δ as a function of the scale k for the four $f(R)$ models considered here. We depict as well the current value of the matter overdensity for a Λ CDM universe. Notice that, for the choice of parameters which ensure an acceptable H_0 ,

[†]In this limit time derivatives are assumed to be negligible with respect to spatial derivatives.

the growth of matter perturbations within the $f(R) = R [\log(\alpha R)]^q - R$ model is highly suppressed with respect to the growth in a universe with a CC. For the other three $f(R)$ models the growth is very close to the Λ CDM growth at large scales. However, it shows a k dependence as k increases, due to a larger $Q(k, a)$ factor, see Eq. (2.13). Galaxy surveys provide information on f , where f is the logarithmic derivative of the linear growth rate, i.e. $f \equiv \frac{d \ln \delta}{d \ln a}$. Therefore for our numerical analyses we will use $f = (\delta'/\delta) a$, see the details in the next section.

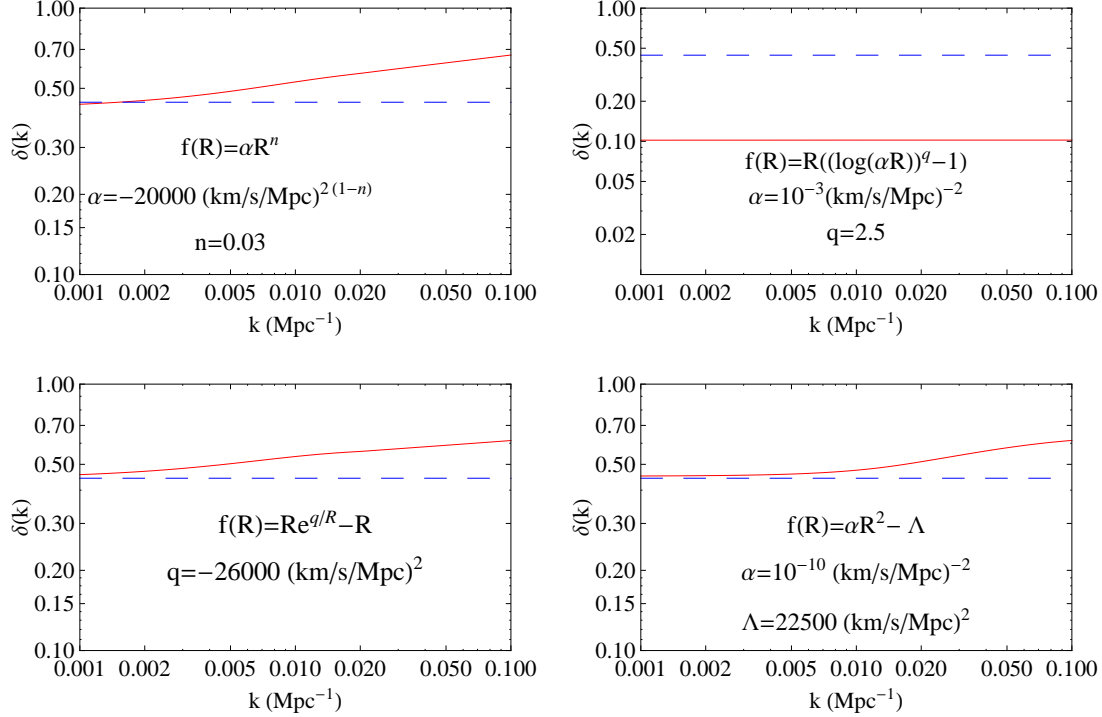


Figure II: Linear growth rate of various $f(R)$ models. The red solid curves depict the present linear overdensity δ as a function of the scale k for the $f(R)$ models explored in this work. The parameters were chosen so to have an acceptable expansion history. We have added the Λ CDM model $\delta(k)$ (blue dashed curve) for comparison.

3. Cosmological data used in the analysis

In this section we describe the cosmological data used in our numerical analyses[‡]. Four different geometrical probes (SNIa, CMB, BAO and $H(z)$ galaxy ages datasets) will be combined with growth of structure data to derive the cosmological bounds on the free parameters of the $f(R)$ models explored here, see Eqs. (2.3), (2.4), (2.5) and (2.6).

[‡]For practical purposes, in the following, we will use the redshift z instead of the scale factor a .

3.1 The Supernova Union Compilation

The Union Compilation [3] is a collection of 414 SNIa, which reduces to 307 SNe after selection cuts. It includes the recent large samples of SNIa from the Supernova Legacy Survey and ESSENCE Survey, and the recently extended dataset of distant supernovae observed with the Hubble Space Telescope (HST). In total the Union Compilation presents 307 values of distance moduli (μ), with relative errors, ranging from a redshift z of 0.05 up to $z = 1.551$. The distance moduli, i.e. the difference between apparent and absolute magnitude of the objects, is given by

$$\mu = 5 \log \left(\frac{d_L}{Mpc} \right) + 25 , \quad (3.1)$$

where $d_L(z)$ is the luminosity distance, $d_L(z) = c(1+z) \int_0^z H(z)^{-1} dz$. The χ^2 function used in the analysis reads

$$\chi_{SNIa}^2(c_i) = \sum_z \left(\frac{(\mu(c_i, z) - \mu_{obs}(z))^2}{\sigma_{obs}^2(z)} \right), \quad (3.2)$$

where, here and in the following, c_i will refer to the free parameters of the f(R) models.

3.2 CMB first acoustic peak

We use here the CMB shift parameter R , since it is the least model dependent quantity extracted from the CMB power spectrum [20], i.e. it does not depend on the present value of the Hubble parameter H_0 . The reduced distance R is written as

$$R = (\Omega_m H_0^2)^{1/2} \int_0^{1089} dz / H(z) . \quad (3.3)$$

The WMAP-5 year CMB data alone yields $R_0 = 1.715 \pm 0.021$ for a fit assuming a constant w [2]. The χ^2 is defined as $\chi_{CMB}^2(c_i) = [(R(c_i) - R_0)/\sigma_{R_0}]^2$.

3.3 BAOs

An independent geometrical probe are BAO measurements. Acoustic oscillations in the photon-baryon plasma are imprinted in the matter distribution. These BAOs have been detected in the spatial distribution of galaxies by the SDSS [21] at a redshift $z = 0.35$ and the 2dF Galaxy Redshift Survey [22] at a redshift $z = 0.2$. The oscillation pattern is characterized by a standard ruler, s , whose length is the distance sound can travel between the Big Bang and recombination and at which the correlation function of dark matter (and that of galaxies, clusters) should show a peak. While future BAO data is expected to provide independent measurements of the Hubble rate $H(z)$ and of the angular diameter distance $D_A(z) = d_L(z)/(1+z)$ at different redshifts, current BAO data does not allow to measure them separately, so they use the spherically correlated function

$$D_V(z) = \left(D_A^2(z) \frac{cz}{H(z)} \right)^{1/3} . \quad (3.4)$$

In Ref. [23], a tension among SDSS and BAO datasets was claimed. Therefore, we will focus on the SDSS dataset in the following. The SDSS team reports its BAO measurements in terms of the A parameter,

$$A(z = 0.35) \equiv D_V(z = 0.35) \frac{\sqrt{\Omega_m H_0^2}}{0.35c} , \quad (3.5)$$

where $A_{SDSS}(z = 0.35) = 0.469 \pm 0.017$. The χ^2 function is defined as $\chi_{BAO}^2(c_i) = [(A(c_i, z = 0.35) - A_{SDSS}(z = 0.35))/\sigma_{A(z=0.35)}]^2$.

3.4 Galaxy ages

We use the $H(z)$ data extracted from galaxy ages in the redshift range $0.1 < z < 1.8$, see Ref. [24]. The authors first selected galaxy samples of passively evolving galaxies with high-quality spectroscopy. Second, they used synthetic stellar population models to constrain the age of the oldest stars in the galaxy (after marginalising over the metallicity and star formation history) and then computed *differential* ages and used them as their estimator for dz/dt , which in turn gave $H(z)$. We use the eight data points shown in Figure 1 in Ref. [24] to test cosmological models by these data sample. The χ^2 function is defined as

$$\chi_{ages}^2(c_i) = \sum_z \left(\frac{(H(c_i, z) - H(z))^2}{\sigma_{H(z)}^2} \right) . \quad (3.6)$$

3.5 Growth factor

Galaxy surveys measure the redshift of the galaxies, providing, therefore, the redshift space galaxy distributions. From those redshifts the radial position of the galaxy is extracted. However, the inferred galaxy distribution (and, consequently, the power spectrum) is distorted with respect to the true galaxy distribution, because in redshift space one neglects the peculiar velocities of the galaxies. These are the so called *redshift space distortions*.

In linear theory and with a local linear galaxy bias b the relation between the true spectrum in real space and the spectrum in redshift space reads

$$P_{\text{redshift}}(\mathbf{k}) = (1 + \beta \mu_{\mathbf{k}}^2)^2 P(\mathbf{k}) , \quad (3.7)$$

where $\beta \equiv f/b$, being f the logarithmic derivative of the growth factor, and $\mu_{\mathbf{k}}$ is the cosine of the angle between the line of sight and the wavevector \mathbf{k} . Notice that perturbations with \mathbf{k} perpendicular to the line of sight are not distorted. By averaging over all directions $\mu_{\mathbf{k}}$, one obtains the relation

$$P_{\text{redshift}}(k) = \left(1 + \frac{2}{3}\beta + \frac{1}{5}\beta^2 \right) P(k) . \quad (3.8)$$

The relation among real space and redshift space overdensities given by Eq. (3.7) was first derived by Kaiser [25] and it arises from the continuity equation, which relates the divergence of the peculiar velocity with the linear matter overdensity. Redshift space distortions, then, relate peculiar velocities with the growth factor f . A measurement of $\beta \equiv f/b$ will provide information on the growth of structure formation if the galaxy bias b

z	β	b	f	References
0.15	0.49 ± 0.09	1.04 ± 0.11	0.51 ± 0.11	[27, 28]
0.35	0.31 ± 0.04	2.25 ± 0.08	0.7 ± 0.18	[4]
0.55	0.45 ± 0.05	1.66 ± 0.35	0.75 ± 0.18	[29]
0.77	0.70 ± 0.26	1.30 ± 0.10	0.91 ± 0.36	[30]

Table 1: Current available data for the redshift distortion parameter β , the bias b and the inferred growth factor, see Ref. [31].

is known. One can estimate the redshift distortion parameter β both by using the ratio of the redshift space correlation function to the real space correlation function, see Eq. (3.8) and by exploiting the ratio of the monopole and quadrupole harmonics of the redshift correlation function [26]:

$$Q_{\text{redshift}} = \frac{P_{\text{redshift}}^{(2)}(k)}{P_{\text{redshift}}^{(0)}(k)} = \frac{\frac{4}{3}\beta + \frac{4}{7}\beta^2}{1 + \frac{2}{3}\beta + \frac{1}{5}\beta^2}. \quad (3.9)$$

We quote the current available data on β , the galaxy bias b and the inferred growth factor in Tab. 1. Notice from the first of Eqs. (2.10) that the continuity equation in $f(R)$ theories is exactly the same than in general relativity and therefore the relation between peculiar velocities and the matter overdensity is not modified in the $f(R)$ models studied here. Consequently, we use the available data on the logarithmic derivative of the growth factor f , see Tab. 1 as an additional test for $f(R)$ models, to be added to the geometrical probes previously described. The χ^2 function is defined as $\chi_{\text{growth}}^2 = \sum_j [(f(c_i, z_j, k_0) - f(z_j))/\sigma_{f(z_j)}]^2$. Notice that the theoretical prediction for the growth factor $f(c_i, z_j, k)$ is scale dependent. We choose $k_0 = 0.1 \text{ Mpc}^{-1}$ to be within the linear regime and within the scale range tested by current surveys, see Tab. 1.

4. Analysis of cosmological models

In this section we present the constraints in four modified gravity models (see Eqs. (2.3) to (2.6)) which arise from the datasets described in the previous section. These models have been shown to have a long enough matter domination epoch and late-time accelerated expansion [17].

We show below that the combination of geometrical probes (i.e. distance measurements) and growth of structure data allows to exclude some models. For those consistent with all the cosmological data sets used here, we derive the allowed range of parameters and discuss the near future improvements. We will see in next section that some of the models consistent with all cosmological data, are excluded by solar system tests.

In the discussion, we make use of the individual chi-square functions, the global chi-square defined by

$$\chi_{\text{tot}}^2(c_i) = \chi_{\text{SNIa}}^2(c_i) + \chi_{\text{BAO}}^2(c_i) + \chi_{\text{CMB}}^2(c_i) + \chi_{\text{ages}}^2(c_i) + \chi_{\text{growth}}^2(c_i),$$

and the *only-distances* χ^2 , defined as the global chi-square without the last term. If not otherwise specified, the cosmological parameters H_0 and Ω_m are fixed to the values 74.2 Km/s/Mpc and 0.24 respectively.

4.1 Model H1: $f(R) = \alpha R^n$ ($\alpha < 0$, $0 < n < 1$)

This model contains two parameters: the power index of the curvature n and the normalization of the modification of gravity α . The αR^n model contains the Λ CDM universe as a limiting case: if $n \rightarrow 0$, then $f(R) \rightarrow \alpha$, where the parameter α becomes a cosmological constant. Therefore, it must be allowed by the cosmological data within a parameter range. The best fit model is acceptable for all the independent data sets and the full data analysis gives a χ^2_{min} of 325.3 for 322 d.o.f.

We firstly discuss the larger n allowed, and how much α deviates from the cosmological constant present in a Λ CDM universe. In Fig. III we show the 68.3, 95.4 and 99.7% CL contours (full colour) resulting from a fit to all the cosmological data exploited here. The global best fit point is marked by a star. Notice that the power index n can be quite large and that the normalization α can depart from the cosmological constant value. In fact, data prefer $n = 0.11$ and $\alpha = -6600 \text{ (km/s/Mpc)}^{2 \times (1-0.11)}$, far from the cosmological constant ($\bar{\Lambda}$) limiting case ($\alpha = -2\bar{\Lambda} \sim -20000 \text{ (km/s/Mpc)}^2$ and $n = 0$).

The regions allowed by growth of structure data are depicted by dashed lines, with the best fit point marked as a plus sign. The allowed regions from a fit to distance measurements (i.e. geometrical probes) are depicted by black lines. The statistical power is dominated by distance data: only an expert eye can notice the difference among the global analysis allowed regions and those coming from the *only-distances* analysis. SNIa data are the most important piece of information that constrains the modified gravity parameters. BAO, CMB and galaxy ages $H(z)$ data sets have a similar weight in the statistical analysis.

Figure III shows some tension between the model predictions and the different data sets for the largest allowed values of n . Notice that additional, high precision growth data may further test the high α region and further constrain the deviations of the $f(R) = \alpha R^n$ model from a Λ CDM universe.

4.2 Model H2: $f(R) = R(\log(\alpha R))^q - R$ ($q > 0$)

This model is described by two parameters: the power index of the logarithm of the curvature q and a normalization of the modification of gravity α . The best fit model is acceptable for the all the distance measurements, with some tension between the allowed ranges derived from the different distance observables.

The relevance of testing this model against cosmological data appears when we compare the allowed regions by geometrical probes to those coming from a fit to growth of structure data: there is no allowed region at more than 99.73% CL able to fit distances and growth data simultaneously, see Fig. IV.

Distance measurements prefer larger values of the power index q , while growth data prefer a much smaller power index. Notice that for parameters that reproduce correctly the expansion history, the linear growth is k -independent but very much off the Λ CDM model (see Figs. I and II). Errors in the inferred growth rate are still large (see Tab. 1),

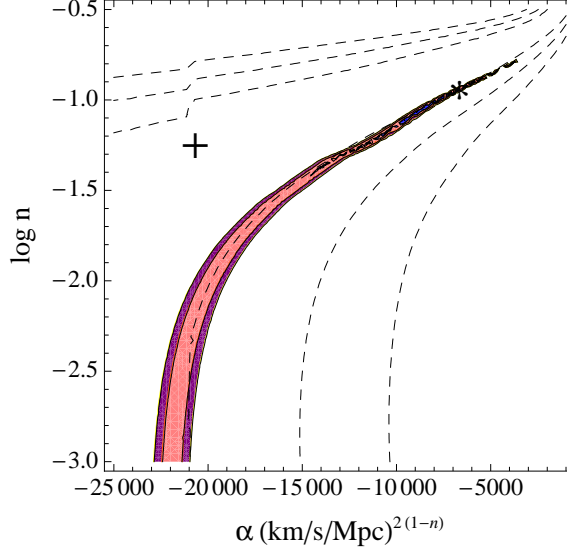


Figure III: Data analysis of model H1. Full regions correspond to the 68.3, 95.4 and 99.7 % CL global analysis allowed regions of parameters n - α of the modified gravity model $f(R) = \alpha R^n$. The best fit point of the global analysis is marked with a star. Dashed lines correspond to the 68.3, 95.4 and 99.7 % CL contours of the growth data analysis. The best fit point of the growth data analysis is marked with a plus sign.

but sufficient to test this model. We obtain $\chi^2_{min} = 388.7$ for 322 d.o.f., with a probability of the result being due to chance $p < 0.006$. Statistically, we can reject the null hypothesis of the model being compatible with data.

4.3 Model H3: $f(R) = R \exp(q/R) - R$

This model contains one free parameter q . We also allow here the current fraction of the energy density in the form of dark matter, Ω_m^0 , to be an additional free parameter.

The $f(R) = R \exp(q/R) - R$ model contains the cosmological constant model as a limiting case. If q/R is small, then $f(R) \rightarrow q$, where the parameter q becomes a cosmological constant. The best fit model is acceptable for all the independent data sets and the full data analysis gives a χ^2_{min} of 332.4 for 322 d.o.f..

Figure V depicts the 68.3, 95.4 and 99.7% CL contours (full colour) resulting from a fit to all the cosmological data exploited here. The parameter q can deviate from the cosmological constant in Λ CDM by less than 10%. From the global analysis we obtain $\Omega_m^0 = 0.245 \pm 0.015$ and $q = -23200 \pm 1200 \text{ (km/s/Mpc)}^2$. The distances only data mostly contributes to strongly constrain the parameter q of this modified gravity model. Notice from Fig. V that the growth data prefer smaller values of q and Ω_m^0 , pushing down the global allowed region respect to the distances only allowed region. Not surprisingly, the best fit of the χ^2_{growth} analysis lies outside the region shown here. Future more accurate growth of structure data could provide tighter bounds on the parameters q and Ω_m^0 , and

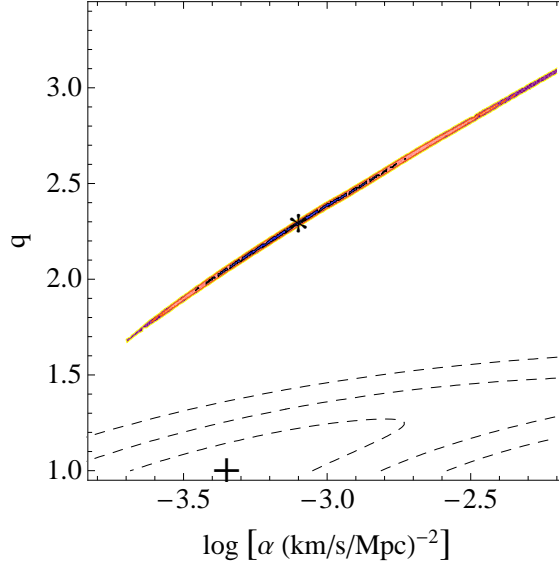


Figure IV: Data analysis of model H2. Full regions correspond to the 68.3, 95.4 and 99.7 % CL distances only analysis allowed regions of parameters q - α of the modified gravity model $f(R) = R(\log(\alpha R))^q - R$. The best fit point of the distances only analysis is marked with a star. Dashed lines correspond to the 68.3, 95.4 and 99.7 % CL contours of the growth data analysis. The best fit point of the growth data analysis is marked with a plus sign.

potentially reject this model if it would not fit simultaneously distances and future growth data.

4.4 Model H4: $f(R) = \alpha R^2 - \Lambda$ ($\alpha\Lambda \ll 1$)

The $f(R) = \alpha R^2 - \Lambda$ ($\alpha\Lambda \ll 1$) model is described by two parameters: the cosmological constant Λ and the normalization of the modification of gravity α . If $\alpha \rightarrow 0$, then $f(R) \rightarrow \Lambda$, a cosmological constant, implying that the model must work in some parameter range. Notice that the Einstein Hilbert action contains the term $R - 2\bar{\Lambda}$, and therefore the Λ is twice the usual cosmological constant $\bar{\Lambda}$. The best fit model is acceptable for all the independent data sets and the full data analysis gives a χ^2_{min} of 323.6 for 322 d.o.f..

Figure VI depicts the 68.3, 95.4 and 99.7% CL contours (full colour) resulting from a fit to all the cosmological data exploited here. The data prefer a very small modification of gravity with $\log[\alpha \text{ (in km/s/Mpc)}^{-2}] < -8$. The best fit point of the global analysis is $\log[\alpha \text{ (in km/s/Mpc)}^{-2}] = -8.23$ and $\Lambda = 23515 \text{ (km/s/Mpc)}^2$, which is about $1\text{-}\sigma$ away from the preferred $\Lambda = 2\bar{\Lambda}$ without a modification of gravity (i.e. $\alpha = 0$). High precision future geometrical probes can reduce the model to a negligible perturbation of the Λ CDM model.

5. Solar system constraints

We explore here the weak field limit of $f(R) = \alpha R^n$, $f(R) = \alpha R^2 - \Lambda$ and $f(R) =$

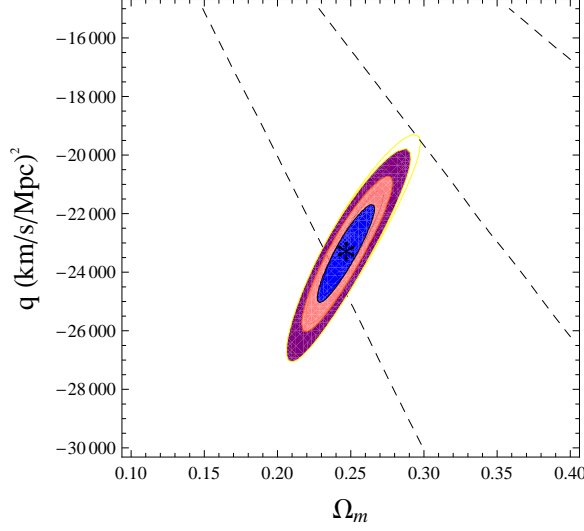


Figure V: Data analysis of model H3. Full regions correspond to the 68.3, 95.4 and 99.7 % CL global analysis allowed regions of parameters q - Ω_m^0 of the modified gravity model $f(R) = R \exp(q/R) - R$. The best fit point of the global analysis is marked with a star. Dashed lines correspond to the 68.3, 95.4 and 99.7 % CL upper part of the contours of the growth data analysis.

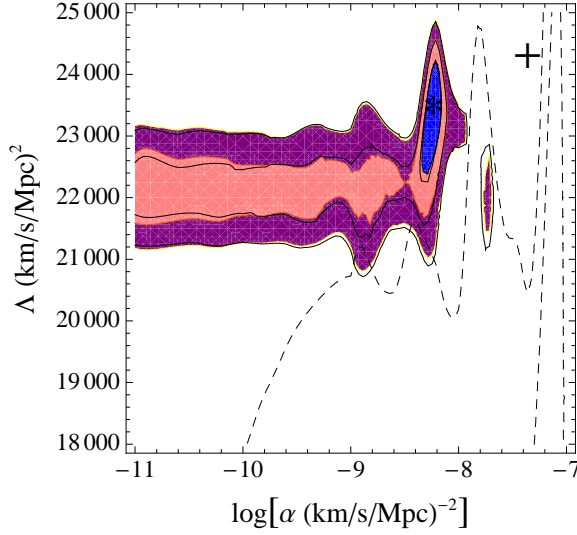


Figure VI: Data analysis of model H4. Full regions correspond to the 68.3, 95.4 and 99.7 % CL global analysis allowed regions of parameters n - α of the modified gravity model $f(R) = \alpha R^2 - \Lambda$ ($\alpha\Lambda \ll 1$). The best fit point of the global analysis is marked with a star. Dashed lines correspond to the 68.3, 95.4 and 99.7 % CL contours of the growth data analysis. The best fit point of the growth data analysis is marked with a plus sign.

$R \exp(q/R) - R$, modified gravity models which have been shown to be consistent with the cosmological probes used in the previous section.

It is well known that $f(R)$ gravity models that produced late time acceleration also have problems to pass solar system tests [32–42]. The reason is that $f(R)$ gravity theories introduce a scalar degree of freedom given by f_R that, for the background cosmological density, is very light. As a consequence, it produces a long-range fifth force, leading to a dissociation of the space-time curvature from the local density. Then, the metric around the sun is predicted to be different than what is observed. Chiba [43] has shown under which conditions an $f(R)$ gravity is equivalent to a scalar-tensor theory with Parametrized Post-Newtonian (PPN) parameter $\gamma = 1/2$, far outside the range allowed by observations, $|\gamma - 1| < 2.310^{-5}$ [44].

However, some $f(R)$ theories are still viable: the scalar field mass could be large and therefore it would not have an effect at solar system scales. Another possibility is a scale dependent scalar field mass, as in the chameleon mechanism [45–49]. In chameleon cosmologies, the effective mass of the scalar field becomes very large in high density environments (as in the Sun’s interior) and the induced fifth force range would be below the detectability level of gravitational experiments.

In what follows we will apply the criteria presented by Hu and Sawicki in Ref. [38]. If the system’s density (for instance, the Sun’s density) changes on scales that are much larger than the scalar field Compton wavelength

$$\lambda_{f_R} \equiv m_{f_R}^{-1}, \quad (5.1)$$

where

$$m_{f_R}^2 = \frac{1}{3} \left(\frac{1 + f_R}{f_{RR}} - R \right), \quad (5.2)$$

the curvature will follow the Sun’s density, as in general relativity. This is the *Compton* condition. If it is satisfied at all radii, high densities will be associated with high curvature and deviations from general relativity will be highly suppressed. If the *Compton* condition is not satisfied, one would need then to check the *thin-shell* condition. This condition applies when the (massive) scalar field is trapped within the system and its influence is only due to a thin shell, shielding the fifth force mediated by the scalar field. For the solar system, the *thin shell* criterion reads [38, 47]

$$|\Delta f_R(r_\odot)| < (\gamma - 1) \frac{GM_\odot}{r_\odot} < 4.9 \times 10^{-11}, \quad (5.3)$$

where Δf_R is the field f_R difference from far inside the body to very far away. Local gravity constraints for the model H1, $f(R) = \alpha R^n$ have been already studied in [40], where it is found that only $n < 5 \times 10^{-6}$ is allowed. Such values of n are too close to Λ CDM, and therefore not interesting cosmologically.

We find that the only $f(R)$ model which satisfies the *Compton* condition and therefore satisfies solar system constraints is $f(R) = R \exp(q/R) - R$. The Compton wavelength for this model is $\lambda_{f_R} \simeq \sqrt{\frac{3q^2}{R^3}}$. For the best fit values of $q \sim -20000 \text{ (km/s/Mpc)}^2$ and for

densities corresponding to the solar corona $\rho \simeq 10^{-15} \text{ g/cm}^3$, $\lambda_{f_R} \simeq 10^{-4} r_\odot$. For higher densities, the Compton wavelength is even smaller and therefore the curvature R will follow the density profile inside the Sun, as in general relativity.

The other two $f(R)$ models which survive the cosmological , i.e. $f(R) = \alpha R^n$ and $f(R) = \alpha R^2 - \Lambda$ do not satisfy the *Compton* nor the *thin* shell criteria, and therefore they are ruled out by solar system observations.

6. Discussion

We have studied a class of modified gravity models, which possess a long enough matter domination epoch and late-time accelerated expansion, as identified by the authors of [17]. Both the background evolution and the growth of structure have been computed in these well behaved modified gravity cosmologies. We have confronted the expansion history in these cosmologies with SNIa data, the CMB shift parameter R , the SDSS BAO measurement and the $H(z)$ data derived from galaxy ages. We have also fitted the linear growth of structure in these $f(R)$ models to the growth information derived from redshift space distortions, as a novel approach.

Interestingly, we find that the cosmological data exploited here possess an enormous potential to rule out modified gravity models. $f(R)$ models with a good expansion history like $f(R) = R (\log(\alpha R))^q - R$ badly fail to reproduce the growth measurements and can be statistically rejected with present data.

Other modified gravity models as $f(R) = \alpha R^n$, $f(R) = \alpha R^2 - \Lambda$ and $f(R) = R \exp(q/R) - R$ are allowed by all the cosmological data exploited in this study, and include as a limiting case a Λ CDM universe. We show the allowed range of parameters in these models, finding that modifications of gravity must be small. The bounds presented here could be greatly improved with future high precision growth data.

We have also studied the solar system bounds on the three $f(R)$ models which agree with the cosmological data. The only model which satisfies solar system constraints is $f(R) = R \exp(q/R) - R$. The other two models, although cosmologically viable, are ruled out by solar system observations.

From a global fit (which includes SNIa, CMB, BAO, $H(z)$ galaxy ages and growth data) to the q parameter in the exponential model $f(R) = R \exp(q/R) - R$ and to the current matter energy density Ω_m^0 , we obtain $\Omega_m^0 = 0.245 \pm 0.015$ and $q = -23200 \pm 1200 \text{ (km/s/Mpc)}^2$. Geometrical probes mostly contribute to strongly constrain the parameter q of this modified gravity model, while growth data slightly prefer lower values of both parameters Ω_m^0 and q . In the parameter allowed region where the exponential model differs from the standard CC cosmology, we find that the growth factor is k -dependent, in contrast to the Λ CDM prediction. More precise growth data at small scales, albeit still within the linear regime, will potentially find small deviations from a universe with a CC.

Our study shows, with the exploration of several $f(R)$ models, that the combination of geometrical probes and growth data offers a powerful tool to rule out modified gravity scenarios and/or constrain deviations from the Λ CDM picture. We can anticipate that future growth of structure data in the linear regime, combined with a full analysis including

the nonlinear regime, will have a very important impact in searching for tiny deviations from Einstein gravity.

Acknowledgments

O.M. and N.R. thank the Fermilab theory group for hospitality. This work is supported in part by the Spanish MICINN grants FPA-2007-60323 and AYA2008-03531, the Consolider Ingenio-2010 project CSD2007-00060 and the Generalitat Valenciana grant PROM-ETEO/2009/116. The work of O.M. is supported by a Ramón y Cajal contract.

References

- [1] **WMAP** Collaboration, J. Dunkley *et. al.*, *Five-Year Wilkinson Microwave Anisotropy Probe (WMAP) Observations: Likelihoods and Parameters from the WMAP data*, *Astrophys. J. Suppl.* **180** (2009) 306–329, [[arXiv:0803.0586](#)].
- [2] **WMAP** Collaboration, E. Komatsu *et. al.*, *Five-Year Wilkinson Microwave Anisotropy Probe (WMAP) Observations: Cosmological Interpretation*, *Astrophys. J. Suppl.* **180** (2009) 330–376, [[arXiv:0803.0547](#)].
- [3] M. Kowalski *et. al.*, *Improved Cosmological Constraints from New, Old and Combined Supernova Datasets*, *Astrophys. J.* **686** (2008) 749–778, [[arXiv:0804.4142](#)].
- [4] **SDSS** Collaboration, M. Tegmark *et. al.*, *Cosmological Constraints from the SDSS Luminous Red Galaxies*, *Phys. Rev.* **D74** (2006) 123507, [[astro-ph/0608632](#)].
- [5] W. J. Percival *et. al.*, *The shape of the SDSS DR5 galaxy power spectrum*, *Astrophys. J.* **657** (2007) 645–663, [[astro-ph/0608636](#)].
- [6] R. R. Caldwell, R. Dave, and P. J. Steinhardt, *Quintessential cosmology: Novel models of cosmological structure formation*, *Astrophys. Space Sci.* **261** (1998) 303–310.
- [7] I. Zlatev, L.-M. Wang, and P. J. Steinhardt, *Quintessence, Cosmic Coincidence, and the Cosmological Constant*, *Phys. Rev. Lett.* **82** (1999) 896–899, [[astro-ph/9807002](#)].
- [8] L.-M. Wang, R. R. Caldwell, J. P. Ostriker, and P. J. Steinhardt, *Cosmic Concordance and Quintessence*, *Astrophys. J.* **530** (2000) 17–35, [[astro-ph/9901388](#)].
- [9] C. Wetterich, *The Cosmon model for an asymptotically vanishing time dependent cosmological ‘constant’*, *Astron. Astrophys.* **301** (1995) 321–328, [[hep-th/9408025](#)].
- [10] P. J. E. Peebles and B. Ratra, *Cosmology with a Time Variable Cosmological Constant*, *Astrophys. J.* **325** (1988) L17.
- [11] B. Ratra and P. J. E. Peebles, *Cosmological Consequences of a Rolling Homogeneous Scalar Field*, *Phys. Rev.* **D37** (1988) 3406.
- [12] G. R. Dvali, G. Gabadadze, and M. Porrati, *4D gravity on a brane in 5D Minkowski space*, *Phys. Lett.* **B485** (2000) 208–214, [[hep-th/0005016](#)].
- [13] S. M. Carroll, V. Duvvuri, M. Trodden, and M. S. Turner, *Is cosmic speed-up due to new gravitational physics?*, *Phys. Rev.* **D70** (2004) 043528, [[astro-ph/0306438](#)].
- [14] S. Capozziello, S. Carloni, and A. Troisi, *Quintessence without scalar fields*, *Recent Res. Dev. Astron. Astrophys.* **1** (2003) 625, [[astro-ph/0303041](#)].

- [15] D. N. Vollick, *Curvature Corrections as the Source of the Cosmological Acceleration*, *Phys. Rev.* **D68** (2003) 063510, [astro-ph/0306630].
- [16] S. M. Carroll *et. al.*, *The cosmology of generalized modified gravity models*, *Phys. Rev.* **D71** (2005) 063513, [astro-ph/0410031].
- [17] L. Amendola, R. Gannouji, D. Polarski, and S. Tsujikawa, *Conditions for the cosmological viability of $f(R)$ dark energy models*, *Phys. Rev.* **D75** (2007) 083504, [gr-qc/0612180].
- [18] A. G. Riess *et. al.*, *A Redetermination of the Hubble Constant with the Hubble Space Telescope from a Differential Distance Ladder*, *Astrophys. J.* **699** (2009) 539–563, [arXiv:0905.0695].
- [19] R. Bean, D. Bernat, L. Pogosian, A. Silvestri, and M. Trodden, *Dynamics of Linear Perturbations in $f(R)$ Gravity*, *Phys. Rev.* **D75** (2007) 064020, [astro-ph/0611321].
- [20] Y. Wang and P. Mukherjee, *Robust Dark Energy Constraints from Supernovae, Galaxy Clustering, and Three-Year Wilkinson Microwave Anisotropy Probe Observations*, *Astrophys. J.* **650** (2006) 1, [astro-ph/0604051].
- [21] SDSS Collaboration, D. J. Eisenstein *et. al.*, *Detection of the Baryon Acoustic Peak in the Large-Scale Correlation Function of SDSS Luminous Red Galaxies*, *Astrophys. J.* **633** (2005) 560–574, [astro-ph/0501171].
- [22] W. J. Percival *et. al.*, *Measuring the Baryon Acoustic Oscillation scale using the SDSS and 2dFGRS*, *Mon. Not. Roy. Astron. Soc.* **381** (2007) 1053–1066, [arXiv:0705.3323].
- [23] A. G. Sanchez and S. Cole, *The galaxy power spectrum: precision cosmology from large scale structure?*, *Mon. Not. Roy. Astron. Soc.* **385** (2008) 830–840, [arXiv:0708.1517].
- [24] J. Simon, L. Verde, and R. Jimenez, *Constraints on the redshift dependence of the dark energy potential*, *Phys. Rev.* **D71** (2005) 123001, [astro-ph/0412269].
- [25] N. Kaiser, *Clustering in real space and in redshift space*, *Mon. Not. Roy. Astron. Soc.* **227** (1987) 1–27.
- [26] A. J. S. Hamilton, *Measuring Omega and the real correlation function from the redshift correlation function*, *Astrophys. J.* **385** (Jan., 1992) L5–L8.
- [27] L. Verde *et. al.*, *The 2dF Galaxy Redshift Survey: The bias of galaxies and the density of the Universe*, *Mon. Not. Roy. Astron. Soc.* **335** (2002) 432, [astro-ph/0112161].
- [28] E. Hawkins *et. al.*, *The 2dF Galaxy Redshift Survey: correlation functions, peculiar velocities and the matter density of the Universe*, *Mon. Not. Roy. Astron. Soc.* **346** (2003) 78, [astro-ph/0212375].
- [29] N. P. Ross *et. al.*, *The 2dF-SDSS LRG and QSO Survey: The 2-Point Correlation Function and Redshift-Space Distortions*, astro-ph/0612400.
- [30] L. Guzzo *et. al.*, *A test of the nature of cosmic acceleration using galaxy redshift distortions*, *Nature* **451** (2008) 541–545, [arXiv:0802.1944].
- [31] S. Nesseris and L. Perivolaropoulos, *Testing LCDM with the Growth Function $\delta(a)$: Current Constraints*, *Phys. Rev.* **D77** (2008) 023504, [arXiv:0710.1092].
- [32] T. Chiba, *$1/R$ gravity and scalar-tensor gravity*, *Phys. Lett.* **B575** (2003) 1–3, [astro-ph/0307338].
- [33] I. Navarro and K. Van Acoleyen, *On the Newtonian limit of Generalized Modified Gravity Models*, *Phys. Lett.* **B622** (2005) 1–5, [gr-qc/0506096].

- [34] G. J. Olmo, *Post-Newtonian constraints on $f(R)$ cosmologies in metric and Palatini formalism*, *Phys. Rev.* **D72** (2005) 083505.
- [35] G. J. Olmo, *The gravity lagrangian according to solar system experiments*, *Phys. Rev. Lett.* **95** (2005) 261102, [[gr-qc/0505101](#)].
- [36] S. Capozziello and A. Troisi, *PPN-limit of fourth order gravity inspired by scalar- tensor gravity*, *Phys. Rev.* **D72** (2005) 044022, [[astro-ph/0507545](#)].
- [37] I. Navarro and K. Van Acoleyen, *$f(R)$ actions, cosmic acceleration and local tests of gravity*, *JCAP* **0702** (2007) 022, [[gr-qc/0611127](#)].
- [38] W. Hu and I. Sawicki, *Models of $f(R)$ Cosmic Acceleration that Evade Solar-System Tests*, *Phys. Rev.* **D76** (2007) 064004, [[arXiv:0705.1158](#)].
- [39] G. J. Olmo, *Limit to general relativity in $f(R)$ theories of gravity*, *Phys. Rev.* **D75** (2007) 023511, [[gr-qc/0612047](#)].
- [40] L. Amendola and S. Tsujikawa, *Phantom crossing, equation-of-state singularities, and local gravity constraints in $f(R)$ models*, *Phys. Lett.* **B660** (2008) 125–132, [[arXiv:0705.0396](#)].
- [41] S. Capozziello, A. Stabile, and A. Troisi, *The Newtonian Limit of $F(R)$ gravity*, *Phys. Rev.* **D76** (2007) 104019, [[arXiv:0708.0723](#)].
- [42] S. Tsujikawa, K. Uddin, S. Mizuno, R. Tavakol, and J. Yokoyama, *Constraints on scalar-tensor models of dark energy from observational and local gravity tests*, *Phys. Rev.* **D77** (2008) 103009, [[arXiv:0803.1106](#)].
- [43] T. Chiba, T. L. Smith, and A. L. Erickcek, *Solar System constraints to general $f(R)$ gravity*, *Phys. Rev.* **D75** (2007) 124014, [[astro-ph/0611867](#)].
- [44] C. M. Will, *The confrontation between general relativity and experiment*, *Living Rev. Rel.* **9** (2005) 3, [[gr-qc/0510072](#)].
- [45] J. Khoury and A. Weltman, *Chameleon cosmology*, *Phys. Rev.* **D69** (2004) 044026, [[astro-ph/0309411](#)].
- [46] J. A. R. Cembranos, *The newtonian limit at intermediate energies*, *Phys. Rev.* **D73** (2006) 064029, [[gr-qc/0507039](#)].
- [47] T. Faulkner, M. Tegmark, E. F. Bunn, and Y. Mao, *Constraining $f(R)$ gravity as a scalar tensor theory*, *Phys. Rev.* **D76** (2007) 063505, [[astro-ph/0612569](#)].
- [48] S. Capozziello and S. Tsujikawa, *Solar system and equivalence principle constraints on $f(R)$ gravity by chameleon approach*, *Phys. Rev.* **D77** (2008) 107501, [[arXiv:0712.2268](#)].
- [49] P. Brax, C. van de Bruck, A.-C. Davis, and D. J. Shaw, *$f(R)$ Gravity and Chameleon Theories*, *Phys. Rev.* **D78** (2008) 104021, [[arXiv:0806.3415](#)].